Synthesis of indium sulfide photoanode, its characterization and application for degradation of methylene blue and methyl orange

by Gunawan Gunawan

Submission date: 01-Feb-2021 01:31PM (UTC+0700)
Submission ID: 1498861018
File name: Prosiding_new_pak_gun.pdf (506.49K)
Word count: 3118
Character count: 15226

Synthesis of indium sulfide photoanode, its characterization and application for degradation of methylene blue and methyl orange

IOP Conf. Series: Materials Science and Engineering **959** (2020) 012021 doi:10.1088/1757-899X/959/1/012021

Synthesis of indium sulfide photoanode, its characterization and application for degradation of methylene blue and methyl orange

Gunawan[1,*], A Haris[1] and W Septina[2]
[1] Department of Chemistry, Faculty of Science and Mathematics, Diponegoro University, Jl. Prof. H. Soedarto, S.H.,Tembalang, Semarang 50275, Indonesia
[2] Hawaii Natural Energy Institute, University of Hawai'i at Mānoa (UHM), 1680 East West Road, POST 109 Honolulu, HI 96822, United States

[*] E-mail: gunawan@live.undip.ac.id

Abstract. The researches on methylene blue (MB) and methyl orange (MO) destructions were carried out using indium sulfide (In_2S_3) photoanode in photoelectrocatalytic system. It consisted of In_2S_3 thin film as an anode synthesized by chemical bath deposition (CBD) on FTO and platinum as a cathode. Characterization with EDX showed the presence of In_2S_3 with a composition close to In_2S_3 for 10 min deposition. The In_2S_3 band gap measurement was obtained 2.49 eV. Photocurrent measurement revealed that In_2S_3 had *n*-type semiconductor property. The application of In_2S_3 thin film as photoanode in a photoelectrocatalytic cell for MB and MO treatments gave degradation's yields *ca*. 71 and 55 %, respectively, under illumination with a 20 watt UV lamp, a bias voltage of 0.5 V for 150 min and with sample concentration of 25 mg/L.

1. Introduction

Photoelectrocatalytic (PEC) cell is a very useful way to treat wastewater organic pollutants that can convert them into non toxic product. Many researchers have focussed this method both for producing electicity and hydrogen generation [1]. The active site of the photoelectrocatalytic cell is anode electrode that made from *n*-type semiconductor, it is called as photoanode, while the cathode electrode is made from platinum. Then, they are immersed in innert solution such as Na_2SO_4, and the electrodes are connected by wire with and without bias potential. Under illumination, photoexitation will be occured at photoanode producing electrons and holes. The electrons generated from this illumination will go from valence band (V_b) to conduction band (V_b), and will flow to external circuit and retured back to catode to reduce water to generate hydrogen. Whereas, the holes producing from photoanode will oxide organic wastes, or react with water or OH^- to form OH^*. The radical of hydroxy (OH^*) is very strong oxidant (2.8V) that can be able to destruct organic wastes resulting carbondioxide, water and other by-products [2].

Now days, several researchers have concerned to series of TiO_2 nanotubes [3–7]. They found photoanode structural properties such as surface area and thickness that affected the ability of the photoanode to utilize light and would hinder the transport of electrons generate by the light [6–8]. Photoanode of ZnO/Zn had been studied with a closed or open circuit system and without using

electolytes [9]. However, the use of electrolytes can increase the performance of photoelectrocatalytic cell [1,10–12] and sodium sulfate is ussually utilized as it is innert electrolyte and it is remained in the solution when photoelectrocatalytic process occurs, since there is no reduction-oxidation reaction taken place for sodium and sulfate ions. The presence of electrolyte in photoelectrocatalytic cell can improve the conductivity of the solution and decrease the internal resistance of the cell. A decrease in internal resistance can cause a larger potential difference at the two electrodes and stimulate the flow of electrons at the cathode, which will leave a hole in the photoanode that is able to oxidize strongly.

Hitherto, there are not much applications of In_2S_3 thin film as a photoanode in a photoelectro-catalytic system. Thin film of In_2S_3 has been widely used as a buffer layer in solar cells [13] and photoelectrochemical water splitting [14–16]. In this research, synthesis of In_2S_3 photoanode for photoelectrocatalytic cell and its application for degradation of methylene blue and methyl orange was conducted. Characterization of the In_2S_3 and its application for destruction of MB and MO with varied electrolytes were studied.

2. Experimental

2.1. (Flourine doped-tin oxide) FTO preparation

Before used for the In_2S_3 deposition, FTO glass was cut into 1 cm x 2 cm and immersed in acetone and sonificated for 10 min. Then soaked into distilled water for 10 min until homogenized with a sonificator. Finally, soaked again in acetone and sonificated for 10 min and it was ready to be used as a glass substrate.

2.2. In_2S_3 Deposition by Chemical Bath Deposition (CBD)

Synthesis of In_2S_3 using CBD method was carried out in an acid cupboard. In 100 mL beaker, 25 mM $InCl_3$, 100 mM thioacetamide and 100 mM acetic acid were added to the beaker, then the FTO was inserted into the beaker vertically using a clamp holder. Furthermore, the magnetic bars were inserted in the beaker and in a water bath on the magnetic strirrer equipped with an electric heater. While stirring at a speed of 100 rpm the bath was heated until the solution in the beaker reached a temperature of 65 ^oC. After about 60 min a yellow deposit of In_2S_3 appeared, and varied deposition times started from this point. Finally, the beaker was removed from the water bath, then the FTO coated with In_2S_3 was taken out and washed with distilled water and dried by spraying with nitrogen gas.

2.3. Characterization

The obtained In_2S_3 thin film was characterized using EDX (Phenom Pro-X desktop SEM with EDX), SEM (JSM-6510LA), XRD (PANalytical X Pert^3 Powder X-ray diffractometer (Cu Kα, Ni filter)), Raman (Jasco NRC 3100 Laser), and determination of the band gap used a UV-Vis spectrophotometer (PG Instruments T60 UV Vis Spectrophotometer), as well as the photocurrent test (*J-V*) with artificial light (1.5 AM solar simulator) in 1 M Na_2SO_3 solution was measured by a potentiostat (Corr Test-150) under chopped irradiation.

2.4. Application of In_2S_3 photoanode for photoelectrocatalysis cell

Dye *w*aste treatment using photoelectrocatalytic cell is schematically showed in figure 1. Photoanode and platinum were assembled and put into the beaker filled with dye to be destructed. Furthermore, the irradiation was carried out using a 20 watt UV lamp (366 nm) and a bias voltage of 0.5 V. The parameters studied in these dye waste treatment processes consisted of the treatment times, the uses of no and varied electrolytes of NaOH, HCl, Na_2SO_4. The dye concentration analysis after the treatment was carried out using a UV-Vis spectrophotometer.

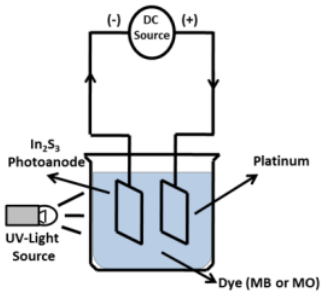

Figure 1. Schematic diagram of dye destrustion using photoelectrocatalytic cell.

3. Results and discussion

The deposition of In_2S_3 on FTO glass is shown in figure 2. It is seen that the thin film was formed evenly on the surface of FTO. A fine film was obtained with 10 min deposition time, and if it was continued, larger In_2S_3 crystals grew to form bulk crystals. However, the presence of bulk crystals will inhibit the semiconductor properties of the photoanode as there was very small photocurrent as it was observed from J-V curve measured by potentiostat.

Figure 2. In_2S_3 thin film deposited on the FTO surface.

3.1. Composition analysis of In_2S_3 thin films with EDX

The composition analysis of In_2S_3 was performed using EDX and shown in table 1 as stated with weight percentages.

Table 1. Percentage of In_2S_3 on FTO glass.

	Weight percentage prepared in		
Element	10 min	20 min	30 min
O	58.00	77.01	50.79
S	12.05	1.26	16.73
In	6.90	0.39	9.88
Sn	23.06	21.34	22.61

From table 1 can be seen that there are 4 elements from the EDX observation, namely oxygen, sulfur, indium and tin. The dominant elements are tin and oxygen. Tin and oxygen come from the constituents of FTO, namely fluorine doped-tin oxide. These observations show that the composition is close to In_2S_3 for the sample prepared at 10 min. This is also supported by the existence of a large photocurrent of the sample (in the next discussion). Although the 10 min sample does not exactly match the percentage of In_2S_3.

3.2. Characterization of the In_2S_3 thin film surface by SEM

Figure 3 shows SEM images of In_2S_3 on FTO with varied times of deposition, it can be seen that the crystals of In_2S_3 have diameters less than 500 nm. Nevertheless. the FTO substrate is not well covered with In_2S_3 thin film precipitate. Even, the SEM is depicted that the film formed does not grow well for

20 min deposition. After 30 min deposition, In_2S_3 crystals form agglomeration not thin film anymore such as in 10 min deposition.

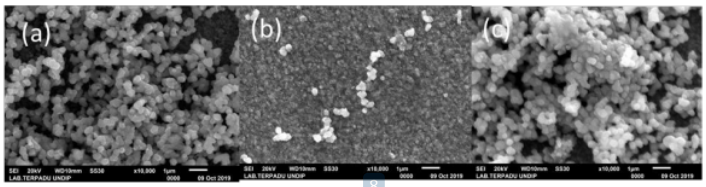

Figure 3. SEM images of In_2S_3 on FTO for deposition times of: (a) 10, (b) 20, and (c) 30 min.

3.3. Analysis In_2S_3 thin film using XRD

Figure 4 shows the X-ray diffraction of In_2S_3 deposited on FTO with a glass support. Because In_2S_3 is amorphous the diffractograms of In_2S_3 samples deposition at varied times do not show any differences. The XRD peaks are dominated by the FTO peaks. The peaks at $2\theta = 34.29^o$, 38.32^o and 62.15^o are the peaks from SnO_2 of the substrate used (FTO).

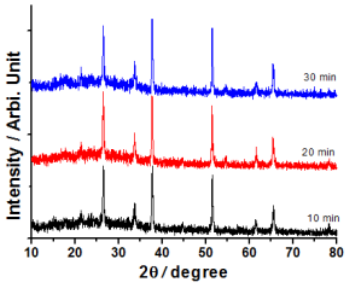

Figure 4. XRD of In_2S_3 thin film on FTO deposited with time variations of 10, 20, 30 min.

3.4. Analysis In_2S_3 with a Raman Spectrophotometer

Raman analysis shows the presence of spectra in the 200 and 300 cm^{-1} shoulder areas which are the typical wave number regions for In_2S_3 as shown in figure 5, namely spectra of In_2S_3 powder and In_2S_3 thin film on glass deposited for 10 min.

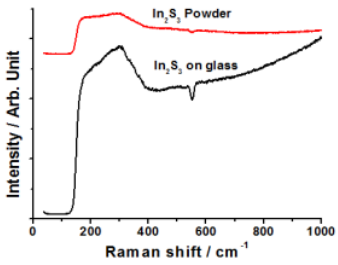

Figure 5. Raman spectra of In_2S_3 powder and In_2S_3 on glass deposited for 10 min.

3.5. Measurement of the absorbance of the In_2S_3 thin film

In_2S_3 thin film deposited for 10 min was then passed through the UV-Vis spectrophotometer pathlight to see the absorbance of the In_2S_3 thin film at various wavelengths. Figure 6 shows that the resulting thin film shows transparency of more than 60% in the visible and near infrared regions at wavelengths greater than 500 nm. At shorter wavelengths (below 500 nm) there is a decrease in transparency due to

the photoexitation of the band gap (E_g). Furthermore, by calculation band gap (hυ) using the relationship hυ = 1239/λ and insertion the wavelength value from figure 6 (496.7 nm) the In_2S_3 band gap can be obtained equals 2.49 eV.

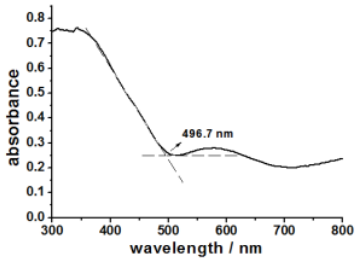

Figure 6. Absorbance *vs* wavelength curve of In_2S_3 thin film at 10 min deposition time.

3.6. Measurement of photocurrent of In_2S_3 thin film

Photocurrent test was done by positioning In_2S_3 photoanode as the working electrode, Ag/ AgCl as the reference electrode and Pt as the counter electrode. Furthermore, to see the presence of photocurrent, the three electrodes were inserted into the 1M Na_2SO_3 solution as a hole scavenger and during the measurement process with the Potentiostat and Galvanostat CS-150 the light was turned off and on to see the difference in photocurrent that occured. Measurements were made from potentials of 0.8 to -0.8 volts. Figures 7a, b, c show the resulting In_2S_3 thin film has a *n*-type semiconductor property. For 10 min deposition, In_2S_3 gives a better photocurrent profile compared to the 20 and 30 min depositions which is indicated by a higher and flatter dark pattern and light current. At a potential of 0.5 V gives a photocurrent ca. 0.01 mA/cm^2 for In_2S_3 deposited for 10 min. Further, application of In_2S_3 thin film deposited for 10 min as a photoanode for dye destruction was used, since it has a better photocurrent.

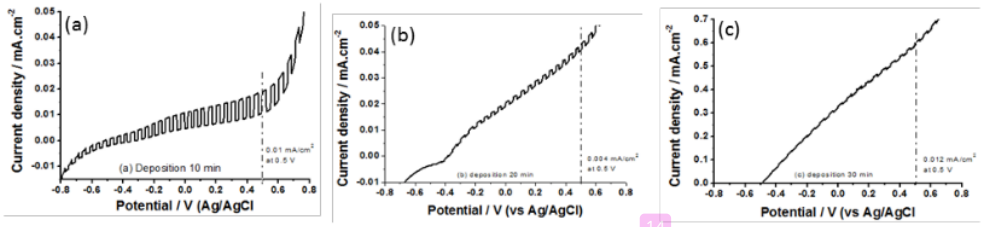

Figure 7. J-V curves for In_2S_3 thin films deposited for (a) 10, (b) 20, (c) 30 min.

3.7. Application of the In_2S_3 thin film as a photoanode for the destruction of MB and MO

The application of the In_2S_3 thin film photoanode deposited for 10 min in a photoelectrocatalytic cell to degrade MB and MO was carried out by irradiation with a 20 watt UV lamp (366 nm) at a distance of 20 cm and a bias voltage of 0.5 V. Figure 8 shows degradation of MB without and with the addition of 0.1M electrolytes of sodium sulfate, NaOH and HCl, respectively with In_2S_3 photoanode for 2.5 h with a bias voltage of 0.5 V. From this figure can be seen MB without using electrolytes provides the smallest decrease in treatment compared to using electrolytes. Whereas the use of HCl provides the smallest reduction compared to sodium sulfate and NaOH electrolytes. When NaOH electrolyte used gave the greatest treatment close to 71% for 150 min. The presence of hydroxide ions in solution increases a further possible methylene blue destruction to occur.

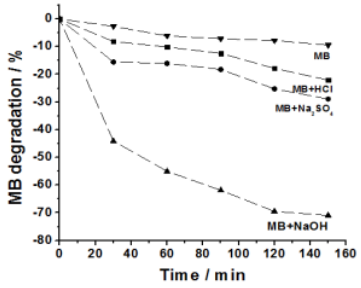

Figure 8. Degradations of MB without and with electrolytes (Na_2SO_4, NaOH and HCl) treated using In_2S_3 photoanode with a bias voltage of 0.5 V.

Methyl orange (MO) was also treated in the similar ways as with MB and the results with varied electrolytes as shown in figure 9.

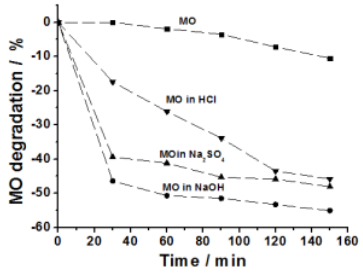

Figure 9. Degradations of MO without and with electrolytes (Na_2SO_4, NaOH and HCl) treated using In_2S_3 photoanode with a bias voltage of 0.5 V.

Figure 9 shows that the treatment patterns are similar when using MO compared to MB although the greatest destruction occurred only up to 55%. This can be the structure of MO is more complicated than that of MB, so it takes a longer process to break down into a smaller molecules.

3.8. UV-Vis measurements of MB and MO at varied electrolytes

UV-Vis measurements of MB and MO were adjusted according to the electrolyte used, because the maximum wavelength is greatly influenced by the type of electrolyte used, as shown in figure 10. Therefore, the reduced MB and MO absorbances after photoelectrocatalytic processes were measured based on the related wavelength of the sample's electrolyes applied. Figure 10a shows that MB gives the same maximum peaks for MB, MB with HCl and Na_2SO_4 and gives a different maximum peak for MB with NaOH. However, for MO with HCl (figure 10b) gives a different maximum peak compared to other treatments that give similar maximum peaks namely for MO with NaOH, Na_2SO_4 electrolytes and without electrolyte.

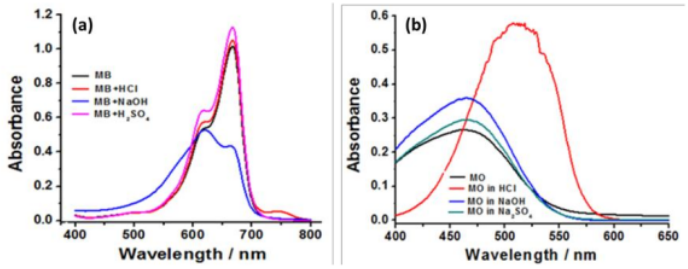

Figure 10. Curve profiles for MB (a) and MO (b) measured without and by using electrolytes (HCl, Na_2SO_4 and NaOH).

4. Conclusion

The synthesis of In_2S_3 thin film by chemical bath deposition (CBD) had been successfully carried out. Characterization with EDX obtained the In_2S_3 composition close to 10 min deposition. SEM image revealed that it did not provide much information regarding In_2S_3 deposition, but for 30 min deposition gave agglomeration deposition. XRD analysis showed the presence of amorphous In_2S_3 which had sharp peaks. From absorption measurement of In_2S_3 thin film deposited for 10 min could be derive a band gap of 2.49 eV. A *n*-type semiconductor property was showed by photocurrent test of In_2S_3 thin film. Application of In_2S_3 deposited 10 min as a photoanode in a photoelectrocatalyst cell for methylene blue and methyl orange treatments resulted degradations up to 71 and 55 %, respectively, for 25 mg /L samples for 2.5 h.

Aknowledgement

The authors were thankful to the Faculty of Science and Mathematics at Diponegoro University for supporting this work (Non APBN FSM UNDIP 2019).

References

[1] Antoniadou M, Kondarides DI, Labou D, Neophytides S and Lianos P 2010 *Sol. Energy. Mater. Sol. Cells* **94** 592
[2] Konstantinou IK and Albanis TA 2004 *Appl. Catal. B Environ.* **49** 1
[3] Liu Y, Zhou B, Li J, Gan X, Bai J and Cai W 2009 *Appl. Catal. B Environ.* **92** 326
[4] Liu Y, Li J, Zhou B, Chen H, Wang Z and Cai W 2011 *Chem. Commun. (Camb)* **47** 10314
[5] Liu Y, Li J, Zhou B, Li X, Chen H, Chen Q, Wang Z, Li L, Wang J and Cai W 2011 *Water Res.* **45** 3991
[6] Li J, Chen Q, Bai J and Zhou B 2013 *J. Hazard. Mater.* **262** 304
[7] Li K, Xu Y, He Y, Yang C, Wang Y and Jia J 2013 *Environ. Sci. Technol.* **47** 3490
[8] Liu Y, Zhou B, Bai J, Li J, Zhang J, Zheng Q, Zhu X and Cai W 2009 *Appl. Catal. B Environ.* **89** 142
[9] Lee SL, Ho IN, Ong SA, Wong YS, Voon CH, Khalik WF, Yusoff NA and Nordin N 2017 *Chemosphere* **166** 118
[10] Wang B, Zhang H, Hu XY, Xuan J and Leung MKH 2014 *Chem. Eng. J* **253** 174
[11] Yang J, Liao W, Liu Y, Muruganathan M and Zhang Y 2014 *Electrochim. Acta* **144** 7
[12] Li L, Xue S, Chen R, Liao Q, Zhu X, Wang Z, He X, Feng H and Cheng X 2015 *Electrochim. Acta* **182** 280
[13] Jiang F, Ozaki C, Gunawan, Harada T, Tang Z, Minemoto T, Nose Y and Ikeda S *Chem. Matter.* **28** 3283
[14] Gunawan G, Septina W, Ikeda S, Harada T, Minegishi T, Domen K and Matsumura M 2014 *Chem. Commun.* **50** 8941
[15] Gunawan, Septina W, Harada T, Nose Y and Ikeda S 2015 *ACS App. Mater. Interfaces* **7** 16086
[16] Jiang F, Gunawan, Harada T, Kuang Y, Minegishi T Domen K and Ikeda S 2015 *J. Am. Chem. Soc.* **137** 13691

Synthesis of indium sulfide photoanode, its characterization and application for degradation of methylene blue and methyl orange

ORIGINALITY REPORT

6%	4%	5%	1%
SIMILARITY INDEX	INTERNET SOURCES	PUBLICATIONS	STUDENT PAPERS

PRIMARY SOURCES

1	Pan, Jiaqi, Jing Li, Xiufang Zhang, Yingying Zheng, Can Cui, Zhiyan Zhu, and Chaorong Li. "The visible light photocatalytic activity enhancement of cotton cellulose nanofibers/In2S3/Ag–CdS nanocomposites", Journal of Physics D Applied Physics, 2016. Publication	1%
2	Xiao-He Liu, Zhong-Hang Xing, Qing-Yun Chen, Yun-Hai Wang. "Multi-functional photocatalytic fuel cell for simultaneous removal of organic pollutant and chromium (VI) accompanied with electricity production", Chemosphere, 2019 Publication	1%
3	pubs.rsc.org Internet Source	1%
4	Claudia Coughlan, Maria Ibáñez, Oleksandr Dobrozhan, Ajay Singh, Andreu Cabot, Kevin	1%

	M. Ryan. "Compound Copper Chalcogenide Nanocrystals", Chemical Reviews, 2017 Publication	
5	www.genchemistry.org Internet Source	1 %
6	Thi Hiep Nguyen, Takato Kawaguchi, Jakapan Chantana, Takashi Minemoto, Takashi Harada, Shuji Nakanishi, Shigeru Ikeda. " Structural and Solar Cell Properties of a Ag-Containing Cu ZnSnS Thin Film Derived from Spray Pyrolysis ", ACS Applied Materials & Interfaces, 2018 Publication	<1 %
7	repositorio.ufscar.br Internet Source	<1 %
8	eprints.usm.my Internet Source	<1 %
9	Ying-Chu Chen, Hao-Hsuan Chang, Yu-Kuei Hsu. " Synthesis of CuInS Quantum Dots/In S /ZnO Nanowire Arrays with High Photoelectrochemical Activity ", ACS Sustainable Chemistry & Engineering, 2018 Publication	<1 %
10	hdl.handle.net Internet Source	<1 %
11	Kané Rabé, Lifen Liu, Noor Ahmed Nahyoon. "Electricity generation in fuel cell with light	<1 %

and without light and decomposition of tetracycline hydrochloride using g-C3N4/Fe0(1%)/TiO2 anode and WO3 cathode", Chemosphere, 2020
Publication

12	www.oasisscientific.com Internet Source	<1 %
13	Asad Mumtaz, Norani Muti Mohamed, Muhammad Mazhar, Muhammad Ali Ehsan, Mohamed Shuaib Mohamed Saheed. " Core–Shell Vanadium Modified Titania@β-In S Hybrid Nanorod Arrays for Superior Interface Stability and Photochemical Activity ", ACS Applied Materials & Interfaces, 2016 Publication	<1 %
14	Huan Wang, Jiyun Feng, Xijun Hu, Ka Ming Ng. "Synthesis of Aligned Carbon Nanotubes on Double-Sided Metallic Substrate by Chemical Vapor Deposition", The Journal of Physical Chemistry C, 2007 Publication	<1 %
15	Tapia, Cristina, Sonia Zacarias, Inês Antunes Cardoso Pereira, José C. Conesa, Marcos Pita, and Antonio L. De Lacey. "In Situ Determination of Photobioproduction of H2 by In2S3-[NiFeSe] Hydrogenase from Desulfovibrio Vulgaris Hildenborough Using Only Visible Light.", ACS Catalysis	<1 %

	Publication	
16	onlinelibrary.wiley.com Internet Source	<1%

Exclude quotes	Off	Exclude matches	Off
Exclude bibliography	Off		

Synthesis of indium sulfide photoanode, its characterization and application for degradation of methylene blue and methyl orange

GRADEMARK REPORT

FINAL GRADE

/0

GENERAL COMMENTS

Instructor

PAGE 1

PAGE 2

PAGE 3

PAGE 4

PAGE 5

PAGE 6

PAGE 7

PAGE 8